Dispersion of plane wave propagation in periodic poroelastic materials : a comparison between Bloch-based and homogenization approaches

V.-H. Nguyen [a], E. ROHAN[b], S. NAILI [a]

a. Université Paris Est Créteil, Laboratoire Modélisation et Simulation Multi Echelle, MSME UMR 8208 CNRS, France

b. NTIS-New Technologies for Information Society, Faculty of Applied Sciences, University of West Bohemia, Czech Republic

Abstract :

This paper aims to study the dispersion phenomena of acoustic waves propagating in a medium composed of a periodic mixture of different poroelastic saturated materials. At mesoscale, each poroelastic saturated material are assumed to be considered by the Biot model. We will present and compare two computational procedures for estimating the effective phase velocities and attenuation of plane waves in the period poroelastic structure at the macroscopic scale. First, wave-based Bloch analysis was employed to derive a finite element formulation which leads to a quadratic complex eigenvalue problem. The equivalent fast/slow compressional as well shear wave modes may be selected by analyzing the computed complex wave numbers. Second, we used the asymptotic homogenization method to derive the effective properties (mass, poroelastic, dynamic permeabilities) which allows us to estimate the effective wave dispersion equation. The polarization of wave modes at the cell level may be reconstructed from macroscopic solution. Numerical results show that both methods could provide well-matched estimations of the effective phase velocities and attenuation within the first Brillouin zone associated with the periodic structure.

Mots clefs : wave dispersion, periodic, poroelastic, Bloch wave, homogenization, finite element

1 Introduction

The analysis of wave propagation in poroelastic media is of great interest in many engineering disciplines such as geophysics, petroleum, biomedical engineering, construction or vehicle materials, etc. The Biot theory [1] has been used in many studies of the dynamic behavior of many kinds of natural materials (rocks, soils, foam, biological tissues (wood and bone)) or synthetic materials (foams, ceramics). However, the dispersion phenomenon has not yet been fully investigated in the situations in which the medium is not homogeneous but heterogeneous at the mesoscale.

This study aims to study the behavior of plane waves propagating in a mesoscopic poroelastic medium in which each REV (Representative Elementary Volume) is a mixture of two different poroelastic materials.

In this study, we distinguish 3 different scales : the microscale which corresponds to the characteristic size (*e.g* pore and skeleton sizes) of both porous materials ; the mesoscopic scale which corresponds to the heterogeneity's size, and macroscale which corresponds to the wavelengths. By assuming that the mesoscopic heterogeneity is much greater that the pore sizes of the porous materials but smaller than wavelengths, the dynamic behavior of each poroelastic material at the mesoscale may be described by using Biot's model. Two methods for computing the wave characteristics (phase velocity and attenuation) at the macroscale have been considered and compared from each to other. First, a Bloch-based finite element formulation is introduced for computing the complex wave numbers in the first Brillouin domain of periodical poroelastic structures with non homogeneous and generic frequency-dependent terms such as the dynamic permeability/tortuosity. Second, a homgenized poroelastic model which was derived by using the two-scale homogenization method was employed. To establish the homogenized model, the effective coefficients are determined by solving the local problems at REV level. The complex wavenumber will be computed by solving the dispersion equation of the homogenized model [6, 5].

2 Biot's poroelastic model

Governing equations. We consider the problem of wave propagation a fluid-saturated anisotropic poroelastic material. To determine the stationary response of the system under an harmonic excitation with angular frequency ω, we assume a time-dependence $e^{\mathrm{i}\omega t}$ for all movement quantities $Y(\boldsymbol{x},t)$, *i.e* $Y(\boldsymbol{x},t) = y(\boldsymbol{x},\omega)e^{\mathrm{i}\omega t}$. In what follows, the term ω in $y(x,\omega)$ will be omitted for simplification purposes.

At each material point $\boldsymbol{x}$ in this medium, the displacement vectors of solid and fluid phases are denoted by $\boldsymbol{u}(\boldsymbol{x})$ and $\boldsymbol{u}^f(\boldsymbol{x})$, respectively. By using Biot's model, the constitutive equations of an anisotropic poroelastic material are given by :

$$\boldsymbol{\sigma} = \mathbb{D} : \boldsymbol{\epsilon} - \boldsymbol{\alpha} p, \tag{1}$$

$$p = -M\left(\boldsymbol{\alpha} : \boldsymbol{\epsilon} + \nabla \cdot \boldsymbol{w}\right), \tag{2}$$

where $\boldsymbol{\sigma}$ and p denote the total stress tensor and the interstitial pore pressure, respectively ; $\boldsymbol{\epsilon}$ denotes the strain tensor : $\boldsymbol{\epsilon} = \frac{1}{2}\left(\nabla \boldsymbol{u} + \nabla \boldsymbol{u}^T\right)$; $\boldsymbol{w}$ is the relative displacement between the fluid and solid phases weighted by the porosity : $\boldsymbol{w} = \phi(\boldsymbol{u}^f - \boldsymbol{u})$ with ϕ is the porosity ; the fourth-order tensor $\mathbb{D}$ denotes the elasticity tensor ; the second-order tensor $\boldsymbol{\alpha}$ is the Biot effective tensor and the scalar M is the Biot's modulus. Neglecting the body forces (other than inertia), the equations describing the linear poroelastic wave propagation in the frequency domain read :

$$-\omega^2 \rho \boldsymbol{u} - \omega^2 \rho^f \boldsymbol{w} - \nabla \cdot \boldsymbol{\sigma} = \boldsymbol{0} \tag{3}$$

$$-\omega^2 \rho^f \boldsymbol{u} - \omega^2 \tilde{\boldsymbol{a}} \boldsymbol{w} + \nabla p = \boldsymbol{0}, \tag{4}$$

where $\rho = \phi\,\rho^f + (1-\phi)\,\rho^s$ is the mixture density, with ρ^s and ρ^f are the solid and fluid mass densities, respectively ; $\tilde{\boldsymbol{a}}$ is the frequency-dependent visco-dynamic second-order tensor which depends on the permeability and tortuosity of the medium :

$$\tilde{\boldsymbol{a}}(\omega) = \frac{\rho^f \boldsymbol{a}^\infty}{\phi} + \frac{\eta}{\mathrm{i}\omega}\,\boldsymbol{k}^{-1}(\omega) \tag{5}$$

where $\boldsymbol{a}^\infty$ is the static tortuosity tensor, η is the fluid's viscosity, and $\boldsymbol{k}$ is the permeability tensor which may be a frequency-dependent tensor.

Weak formulation. Let $\delta\boldsymbol{u}$ and $\delta\boldsymbol{w}$ two vector-valued test functions of $\boldsymbol{u}$ and $\boldsymbol{w}$, respectively, the weak formulation of the problem (Eqs. 3,4) in a domain Ω with the boundary Γ reads :

$$-\omega^2\int_\Omega \delta\boldsymbol{u}\cdot\rho\boldsymbol{u}-\omega^2\int_\Omega \delta\boldsymbol{u}\cdot\rho^f\boldsymbol{w}+\int_\Omega \delta\boldsymbol{\epsilon}:\boldsymbol{\sigma}-\int_\Gamma \delta\boldsymbol{u}\cdot(\boldsymbol{\sigma}\boldsymbol{n}_\Gamma)=\boldsymbol{0} \tag{6}$$

$$-\omega^2\int_\Omega \delta\boldsymbol{w}\cdot\rho^f\boldsymbol{u}-\omega^2\int_\Omega \delta\boldsymbol{w}\cdot\tilde{\boldsymbol{a}}\boldsymbol{w}-\int_\Omega \nabla\cdot(\delta\boldsymbol{w})p+\int_\Gamma \delta\boldsymbol{w}\cdot(p\boldsymbol{n}_\Gamma)=\boldsymbol{0} \tag{7}$$

where n^Γ is the normal unit vector to Γ.

3 Floquet-Bloch wave analysis

Weak formulation for Bloch wave problem. Let us consider an infinite periodic poroelastic domain $\Omega\in\mathbb{R}^d$ whose the lattice is generated by a rectangular parallelepiped primitive cell Ω_E : $\Omega_E=\prod_{j=1}^d]0,\ell_j[$ where d is the dimension of the problem. In this domain, a generic property P satisfies $P(x_j+\ell_j)=P(x_j)$. By considering a primitive cell of the periodic problem and by using the Bloch theorem, the dispersion of plane wave propagation problem this problem can be determined by considering the Floquet-Bloch ansatzs :

$$\boldsymbol{u}(\boldsymbol{x})=\boldsymbol{U}(\boldsymbol{x},\boldsymbol{k})e^{-\mathrm{i}\boldsymbol{k}\cdot\boldsymbol{x}},\qquad \boldsymbol{w}(\boldsymbol{x})=\boldsymbol{W}(\boldsymbol{x},\boldsymbol{k})e^{-\mathrm{i}\boldsymbol{k}\cdot\boldsymbol{x}}, \tag{8}$$

where $\boldsymbol{U}(\boldsymbol{x},\boldsymbol{k})$ and $\boldsymbol{W}(\boldsymbol{x},\boldsymbol{k})$ are Ω_E-periodic function, $\boldsymbol{k}$ is wavenumber vector : $\boldsymbol{k}=k\boldsymbol{n}$, with the unit vector $\boldsymbol{n}$ denotes the wave direction and k is wave number in the direction $\boldsymbol{n}$. Then by applying the test functions $\delta\boldsymbol{u}$ and $\delta\boldsymbol{w}$ of $\boldsymbol{u}$ and $\boldsymbol{v}$, respectively, under the forms :

$$\delta\boldsymbol{u}(\boldsymbol{x})=\delta\boldsymbol{U}(\boldsymbol{x},k)e^{\mathrm{i}k\boldsymbol{n}\cdot\boldsymbol{x}},\qquad \delta\boldsymbol{w}(\boldsymbol{x})=\delta\boldsymbol{W}(\boldsymbol{x},k)e^{\mathrm{i}k\boldsymbol{n}\cdot\boldsymbol{x}}, \tag{9}$$

into Eqs. 6-7, and by applying the periodic condition we obtain the weak formulation written for a cell domain Ω_E :

$$\begin{aligned}-\omega^2\int_{\Omega_E}\delta\boldsymbol{U}\cdot\left(\rho\boldsymbol{U}+\rho^f\boldsymbol{W}\right)+\int_{\Omega_E}\delta\boldsymbol{\mathcal{E}}:\boldsymbol{\Sigma}+\mathrm{i}k\int_{\Omega_E}(\delta\boldsymbol{\mathcal{E}}_n:\boldsymbol{\Sigma}-\delta\boldsymbol{\mathcal{E}}:\boldsymbol{\Sigma}_n)\\ +k^2\int_{\Omega_E}\delta\boldsymbol{\mathcal{E}}_n:\boldsymbol{\Sigma}_n=\boldsymbol{0}\end{aligned} \tag{10}$$

$$\begin{aligned}-\omega^2\int_{\Omega_E}\delta\boldsymbol{W}\cdot\left(\rho^f\boldsymbol{U}+\tilde{\boldsymbol{a}}\boldsymbol{W}\right)-\int_{\Omega_E}(\nabla\cdot\delta\boldsymbol{W})P-\mathrm{i}k\int_{\Omega_E}[(\boldsymbol{n}\cdot\delta\boldsymbol{W})P-(\nabla\cdot\delta\boldsymbol{W})P_n]\\ -k^2\int_{\Omega_E}(\boldsymbol{n}\cdot\delta\boldsymbol{W})P_n=\boldsymbol{0}\end{aligned} \tag{11}$$

in which the functions $\boldsymbol{\mathcal{E}}$, $\boldsymbol{\mathcal{E}}_n$, P, P_n, $\boldsymbol{\Sigma}$, $\boldsymbol{\Sigma}_n$ are expressed by :

$$\boldsymbol{\mathcal{E}}=\{\nabla\boldsymbol{U}\}_s,\quad \boldsymbol{\mathcal{E}}_n=\{\boldsymbol{n}\otimes\boldsymbol{U}\}_s \tag{12}$$

$$P=-M\left[\boldsymbol{\alpha}:\{\nabla\boldsymbol{U}\}_s+\nabla\cdot\boldsymbol{W}\right],\quad P_n=-M\left[\boldsymbol{\alpha}:(\{\boldsymbol{n}\otimes\boldsymbol{U}\}_s)+\boldsymbol{n}\cdot\boldsymbol{W}\right] \tag{13}$$

$$\boldsymbol{\Sigma}=\mathbb{D}^u:\{\nabla\boldsymbol{U}\}_s+M\boldsymbol{\alpha}(\nabla\cdot\boldsymbol{W}),\quad \boldsymbol{\Sigma}_n=\mathbb{D}^u:\{\boldsymbol{n}\otimes\boldsymbol{U}\}_s+M\boldsymbol{\alpha}\left(\boldsymbol{n}\cdot\boldsymbol{W}\right), \tag{14}$$

where $\mathbb{D}^u$ is the undrained elasticity tensor defined by : $\mathbb{D}^u=\mathbb{D}+M\boldsymbol{\alpha}\otimes\boldsymbol{\alpha}$.

Computing the wave numbers using FEM. Applying finite element discretization of the systems of equations (Eqs. 10-11) leads to a nonlinear eigenvalue problem :

$$\left[-\omega^2\mathbf{A}_0(\omega)+\mathrm{i}k\mathbf{A}_1+k^2\mathbf{A}_2\right]\begin{pmatrix}\mathbf{U}^h\\ \mathbf{W}^h\end{pmatrix}=\mathbf{0} \tag{15}$$

where $\mathbf{U}^h$ and $\mathbf{W}^h$ denote the nodal solution of $\boldsymbol{U}$ and $\boldsymbol{W}$, respectively. The expressions of the matrices, which may be derived directly from Eqs. (10-11), are long and not given here.

Noting that the matrix $\mathbf{A}_0$ in (15) contains the dynamic tortuosity tensor which is a frequency-dependent, the dispersion relation will be solved by fixing ω and a direction of wave propagation $\boldsymbol{n}$, then seeking the the solutions of the quadratic eigenvalue problem (15) with respect to k.

In principle, for a given FE-discretized model, one can find $2\times\mathsf{n}_{\mathsf{dof}}$ eigenvalues k, where $\mathsf{n}_{\mathsf{dof}}$ is the number of degrees of freedom. The real parts k^R of the eigenvalues are distributed symmetrically with respect to zero ; a half of these eigenvalues correspond to the waves propagating in direction $+\boldsymbol{n}$, while the other half of the waves propagate in the opposite direction $-\boldsymbol{n}$. Note that the condition of positive dissipation requires $k^Rk^I<0$. We are interested in propagative modes which have the smallest attenuation. Consequently, when solving the eigenvalue problem (15), it is not necessary to determine all $2\times\mathsf{n}_{\mathsf{dof}}$ eigenvalues of the system but only some of them, which have k^I very small. For this reason, when solving the eigenvalue problem, it is more convenient to introduce a new variable $\lambda:=\mathrm{i}k$, so that the most propagative modes correspond the new eigenvalues with the smallest real parts λ^R.

4 Numerical examples

The aim of this section is to illustrate the dispersion analysis of bulk waves propagating in a infinite poroelatic media with mesoscopic heterogeneity, as described above. In particular, we compare the results obtained by the Floquet-Bloch analysis with the corresponding results computed using the homogenized medium model. We consider 2D periodic poroelastic structures with the square REV composed of a circular inclusions (Y_2) and a matrix (Y_1) (see Fig. 1). The size of the REV is given by $\ell_1=\ell_2=1$ mm and the radius of the inclusion is $r=0.25$ mm. Both poroelastic materials in Y_1 and Y_2 are assumed to be isotropic and saturated by water. The mechanical properties of these two poroelastic materials are presented in Fig. 1 (right). In this table, K^b, μ^b denote the drained bulk modulus and the shear modulus of the drained porous materials.

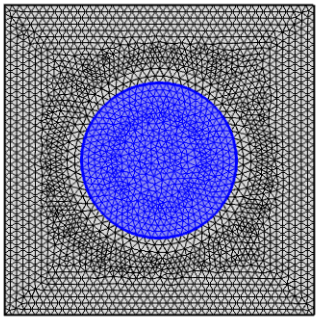

		Rock (Y_1)	**Sandstone** (Y_2)
ρ	kg.m^{-3}	2650	2650
ϕ	-	0.15	0.36
K^b	-	12.7	1.37
μ^b	GPa	20.3	0.82
α	-	0.6825	0.9658
μ	GPa	12.503	5.7096
k_0	m^2	0.1×10^{-12}	1.6×10^{-12}
ρ^f	kg.m^{-3}	1000	1000
K^f	GPa	2.25	2.25
η	Pa.s	10^{-3}	10^{-3}
a_∞	-	1	2.8

FIGURE 1 – Finite element mesh of a square REV ($\ell_1=\ell_2=1$ mm) with circular inclusion ($r=0.25$ mm) ; the subdomains Y_1 and Y_2 are found in gray and blue zones, respectively (left) ; Material parameters in both domains (right)

At each frequency value, we estimate the phase velocities and the dissipation factors of three fundamental wave propagation modes of the effective medium. These modes correspond to the fast quasi-compressional wave (P1-wave), the slow quasi-compressional wave (P2-wave) and the "quasi shear" wave (S-wave). Using a computed complex wave number k, the phase velocity $V_{\text{ph}} = \omega/\text{Re}(k)$ is evaluated, then also the dissipation factor Q^{-1} (which is inverse of the quality factor Q) is introduced by : $Q^{-1} = -2\text{Im}(v_c)/\text{Re}(v_c)$, where $v_c = \omega/\kappa$ is the complex phase velocity. In what follows, we compare the results obtained by the two proposed methods, *i.e* by using the Floquet-Bloch analysis and by using the model of the homogenized medium, the same finite element mesh is employed to discretize the REV by triangular elements with sizes $\sim 0.025\ell$.

Considering plane waves propagating in $\mathbf{e}_1$-direction, we investigate the dispersion of wave modes (P_1, P_2 and S) in a frequency range from 10 Hz to 1 MHz. For the Floquet-Bloch analysis, the model consists of ~ 29.3 thousands DOFs, but we only seek for 30 lowest eigenvalues.

Figures 2a and 2b present the dispersion of phase velocities and the corresponding dissipation factors of the effective P_1, P_2 and S waves with respect to frequency. While the wave velocities of the P_1 and S modes are nearly frequency-independent within the studied frequency range, a significant velocity dispersion is observed for the P_2 mode. On the contrary, the attenuations of the P_1 and S modes, being very small in low frequencies, increase exponentially with frequencies ranging 10 Hz to 100 kHz before reaching the critical frequency. The slow compressional wave P_2 is much more attenuated than two others (P_1 and S), especially at low frequencies.

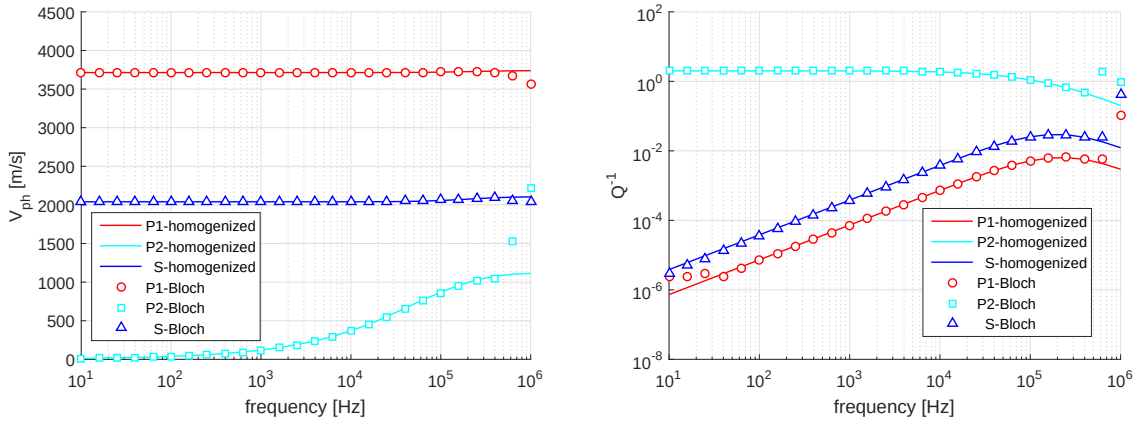

(a) (b)

FIGURE 2 – Case of REV with circular inclusions : Dispersion of (a) phase velocity and (b) dissipation factor of the modes P_1 (fast quasi-compressional wave), P_2 (slow quasi-compressional wave) and S (quasi shear wave) ; wave direction $\mathbf{n} \equiv \mathbf{e}_1$, geometry of REV : $\ell = 1$ mm, $a = b = 0.4$ mm

The comparison shows that the dispersion obtained by the two methods provide results which match very well at almost frequencies in the studied frequency range. The dispersion curves obtained by the Floquet-Bloch analysis diverge from those obtained by the homogenization-based predictions at frequencies greater than $f = 10^5$ Hz. This phenomenon may be explained by comparing the estimated wavelengths of effective modes with the period of the heterogeneity variation, which determines the size ℓ of the RVE and, thereby also the irreducible Brillouin zone. The shortest wavelengths at $f = 10^5$ Hz and at $f = 3.98 \times 10^5$ Hz are the ones of the P_2 modes and equal to $\lambda_{P2} = 8.6$ mm and $\lambda_{P_2} = 2.6$ mm, respectively. At $f = 10^6$ Hz, the S mode presents the smallest wavelength $\lambda_S = 2.03$ mm which, thus,

tends to the limit wave length $\lambda_{\min} = 2\ell = 2$ mm feasible within the irreducible Brillouin zone. Clearly, the homogenization-based wave dispersion analysis is valid for longer wave lengths, $\lambda \gg \lambda_{\min}$.

5 Conclusions

This paper presents a formualtion using Floquet-Bloch wave decomposition (FB) method to analyze the plane wave propagation in periodic poroelastic media. To the best of our knowledge, the Floquet-Bloch decomposition-based analysis of plane waves in poroelastic meadia has not been treated in the literature [2]. The results are compared with the ones obtained by using asymptotic homogenization methods which are previously presented previous works [6, 5].

It has been shown that the homogenization model provides an accurate and computationally quite efficient method to analyze the wave dispersion, when compared to the Bloch method. However, the applicability of the homogenization method is limited to wave lengths which should span at least several periods of the heterogeneous structure to adhere the scale separation assumption.

Further works already in progress concern validation of the homogenized models of fluid saturated porous media with large contrasts in the permeability and poroelastic coefficients [3, 4]

Références

[1] M. Biot. Theory of propagation of elastic waves in a fluid-saturated porous solid. II. Higher-frequency range. *J. Acoust. Soc. Am.*, 28(2) :179–191, 1956.

[2] M. Collet, M. Ouisse, M. Ruzzene, and M. N. Ichchou. Floquet-Bloch decomposition for the computation of dispersion of two-dimensional periodic, damped mechanical systems. *International Journal of Solids and Structures*, 48(20) :2837–2848, 2011. doi : 10.1016/j.ijsolstr.2011.06.002.

[3] V.-H. Nguyen, E. Rohan, and S. Naili. Multiscale simulation of acoustic waves in homogenized heterogeneous porous media with low and high permeability contrasts. *International Journal of Engineering Science*, 101 :92–109, 2016.

[4] E. Rohan, S. Naili, and V.-H. Nguyen. Wave propagation in a strongly heterogeneous elastic porous medium : Homogenization of Biot medium with double porosities. *Comptes Rendus Mecanique*, 344(6) :569–581, 2016.

[5] E. Rohan, V.-H. Nguyen, and S. Naili. Numerical modelling of waves in double-porosity Biot medium. *Computers & Structures*, 2017. (In Press), https ://doi.org/10.1016/j.compstruc.2017.09.003.

[6] E. Rohan, S. Naili, and V.-H. Nguyen. Modelling of waves in fluid-saturated porous media with high contrast heterogeneity : homogenization approach. *ZAMM - Journal of Applied Mathematics and Mechanics / Zeitschrift fÃ¼r Angewandte Mathematik und Mechanik*, 98(9) :1699–1733, 2018.